Hydrometallurgy 191 (2020) 105186

Contents lists available at ScienceDirect

Hydrometallurgy

journal homepage: www.elsevier.com/locate/hydromet

Influence of nettle extract on zinc electrodeposition in an acidic bath: Electrochemical effect and coating morphology

A. Zaabar[a], E. Rocca[b,*], D. Veys-Renaux[b], R. Aitout[a], H. Hammache[a], L. Makhloufi[a], K. Belhamel[c]

[a] Laboratoire d'Électrochimie, Corrosion et de Valorisation Energétique (LECVE), Université de Bejaia, 06000 Bejaia, Algeria
[b] Institut Jean Lamour, Université de Lorraine, Dept CP2S, BP 50840 - Campus Artem, 2 allée André Guinier, 54011 Nancy cedex, France
[c] Laboratoire de Matériaux Organiques (LMO), Université de Bejaia, 06000 Bejaia, Algeria

ARTICLE INFO

Keywords:
Zinc
Electrodeposition
Nettle extract
Electrowinning

ABSTRACT

The electrodeposition of zinc from an acidic sulphate bath was studied in the presence of nettle (*Urtica dioica L.*) extract at room temperature and with relative low zinc concentration. Different electrochemical measurements show that the nettle extract allows a reduction of hydrogen adsorption on steel and zinc and therefore a decrease in hydrogen evolution, due to the specific adsorption of molecules of the extract. Scanning electron microscopy (SEM) observations and X-ray diffraction (XRD) measurements reveal that the addition of nettle extract induces a very fine grain size with a random crystallographic orientation. Finally, the nettle extract constitutes an interesting and low cost additive for all processes based on zinc electrochemical reduction in acidic sulphate electrolytes.

1. Introduction

Electrochemical deposition of zinc is widely used for steel protection against corrosion, due to the sacrificial property of zinc, its low cost, its high availability from industrial waste and the easy implementation of the process. A large selection of organic additives have been studied both to improve the surface morphology of deposits (roughness, porosity, brightness, grain size) and the metallographic structure such as the grain size and the crystallographic orientation of zinc grains (Sorour et al., 2017). The second practical effect of additives is the enhancement of cathodic current efficiency (Youssef et al., 2004; Díaz-Arista et al., 2005; Mouanga et al., 2007; Trejo et al., 2001). In all cases, the germination and growth of zinc grains, which drive the deposit morphology and the current efficiency, mainly depend on the cathodic polarization or depolarization of each electrochemical process.

In the case of zinc electrodeposition, zinc ions are easily reduced with a relative low overpotential in acidic electrolytes. Consequently, without additives, the throwing power is relatively low and coarse crystalline grains of zinc with a rough surface are easily formed. Moreover, H^+ reduction generally occurs in the same potential range as Zn^{2+} reduction process. Therefore, zinc electrodeposition is often accompanied by simultaneous hydrogen evolution reaction, which affects the current efficiency, and can induce the trapping of hydrogen in the substrate or the deposit (Mirkova et al., 2001; Casanova et al., 1997). From the electrochemical point of view, a reaction mechanism has been firstly proposed by Epelboin et al. (Epelboin et al., 1975) which highlights the competitive adsorption of hydrogen, H_{ads}, and zinc cations, Zn^{+}_{ads}, on the surface substrate before the crystallization of zinc metal and the formation of dihydrogen gas.

In industrial applications, the common types of additives are gums, gelatins or glues which are composed by proteins and polysaccharides, and are generally under a cationic form in acidic media (Kerby et al., 1977). Although these compounds are easy to use and nontoxic, many studies report that they have a negative effect on the cathodic polarization of zinc reduction which seems to affect the current efficiency.

Currently, the research of less toxic, low-cost and available additives for electrodeposition process is an important challenge for zinc coating applications but also for zinc electrowinning from liquid waste. Especially, the zinc electrowinning from low zinc concentrated electrolytes at room temperature is challenging because of low current efficiency and bad quality of zinc deposit (Scott et al., 1988). In this context, only a few studies have shown the possibility to use natural compounds as additives in electrolytic or electroless deposition processes (Scott et al., 1988; Loto et al., 2014). In fact, plant extracts have the advantages to be inexpensive, available and renewable materials in many countries and are stable in acidic media (Loto et al., 2014; Mouanga et al., 2008; Zaabar et al., 2014; M'hiri et al., 2016).

The objective of this study is to evaluate the effect of the addition of nettle plant extract on the electrodeposition of zinc in acidic sulfate bath onto carbon steel. The nettle extract (noted NE) was obtained from

* Corresponding author.
E-mail address: emmanuel.rocca@univ-lorraine.fr (E. Rocca).

https://doi.org/10.1016/j.hydromet.2019.105186
Received 22 January 2019; Received in revised form 25 September 2019; Accepted 18 October 2019

Urtica dioica L. plant, with a simple reflux technique in water (Zaabar, 2015). In this work, the electrochemical effects of nettle extract on zinc reduction onto carbon steel were investigated by stationary (potentiodynamic polarizations, chronopotentiometry, chronoamperometry) and dynamic electrochemical techniques (electrochemical impedance spectroscopy). The coating morphology was analyzed using scanning electron microscopy (SEM) and X-ray diffraction (XRD) was used to determine the crystallographic orientations of the zinc deposits.

2. Experimental

Nettle (*Urtica dioica L.*) extract (noted NE) used as additive in zinc deposits was obtained by drying the plant for 24 h in an oven at 40 °C and grinding into powder. A sample of 10 g of the dry powder was extracted by reflux in 100 mL of distilled water for 1 h. The refluxed solution was filtered and 10 mL of the filtrate were evaporated. The resulting solid residue was diluted to prepare a stock solution with a concentration expressed in grams of solid per liter of water ($g\,L^{-1}$). The composition of nettle extract in water was studied by S. Durovic et al., and it is generally composed by polyphenolic compounds, fatty acids (linoleic and palmitic acids), carotenoids compounds and terpenes alcohol (linalool) (Đurovic et al., 2017). This plant is used for a long time in health and food applications due to its antioxidant properties.

The electrochemical measurements were performed without stirring in deaerated conditions, with a three-electrode cell, connected to an PGP 201 Potentiostat/Galvanostat and a frequency response analyzer (PGSTAT30), driven by a computer. In this configuration, the circular working electrode surface (active area: 2.835 cm^2) is vertical, facing the Pt-disk counter electrode (M'hiri et al., 2016). The reference electrode was a K_2SO_4-saturated sulfate electrode (SSE, E = +0.658 V/SHE at 25 °C) and all the working electrode potentials are given versus this reference. As working electrode, both carbon steel XC38 (composition wt%: 0.38% C, 0.66% Mn, 0.25% Cr, 0.02% Mo, 0.27% Si, 0.02% Ni, 0.02% P, 0.016% S, Fe balance) and zinc (99.5 wt%) were studied. Before the experiments, the working electrode was mechanically polished with successively finer grades of SiC emery papers up to P2400. Samples were finally rinsed with distilled water, ethanol and dried. Voltametric studies were carried out from the open-circuit potential to −2 V at 1 $mV\,s^{-1}$ and voltammograms were corrected for ohmic drop. Electrochemical impedance spectroscopy was performed at open-circuit potential with potential magnitude of 10 mV between 100 kHz and 10 mHz.

The plating bath was made of 0.1 M Na_2SO_4, 0.2 M H_3BO_3 (to maintain constant the solution pH), which constitutes the supporting electrolyte, and 0.1 M $ZnSO_4$. The pH value of the solution was adjusted to 2 by adding concentrated sulfuric acid at room temperature (25 °C), and the electrochemical measurements were carried out in deaerated conditions without stirring.

The surface morphology of the deposits was analyzed using scanning electron microscopy (SEM, Philips FEI Quanta 200) and the preferred crystallographic orientation was determined by X-ray diffraction analysis (Expert Prof Panalytical MPD diffractometer).

3. Results and discussion

3.1. Effect of nettle extract on the hydrogen evolution on steel and zinc

To determine the effect of NE on the hydrogen evolution reaction, voltammetric studies and impedance measurements were performed using the supporting electrolyte (0.1 M Na_2SO_4 + 0.2 M H_3BO_3) without zinc salt.

On steel, without NE in the supporting electrolyte, the cathodic polarization curve reveals two first broad cathodic peaks noted C1 and C2 in Fig. 1a, attributed to different processes of proton reduction. According to the literature (Amokrane et al., 2007; Gabe, 1997), these two reduction processes can be assigned to a reduction process via an adsorption step followed by the formation of hydrogen bubbles and a reduction reaction leading to the absorption of hydrogen atoms in steel. The last increase in cathodic current density C3 is clearly attributed to the reduction of protons and water into hydrogen gas on the electrode.

With NE, the cathodic curve shows a decrease in the cathodic current density of H^+ reduction processes (C1 and C2) below −1500 mV from the 1.5 $g\,L^{-1}$ of NE. The effect of NE addition on the C3 reduction process is similar, leading to a decrease in the hydrogen evolution kinetic on the steel surface. The concentration of 1.5 $g\,L^{-1}$ of nettle extract seems to be an optimum value, no significant effect being observed beyond this threshold. Consequently, in stationary and galvanostatic conditions at −3 $mA\,cm^{-2}$, the addition of 1.5 $g\,L^{-1}$ of NE induces a large decrease in the potential of hydrogen evolution of about 300 mV on steel, as illustrated in Fig. 1b.

The Nyquist plot drawn in Fig. 2 shows one capacitive loop without NE, indicating a single charge transfer reaction with a charge transfer resistance of about 300 $\Omega{\cdot}cm^2$. At low frequency, a slight inductive phenomenon can be observed due to the adsorbed hydrogen species on steel. When NE is added to the solution, the impedance diagram clearly reveals both a high-frequency capacitive loop attributed to the charge transfer reaction at the interface with a higher value of the corresponding resistance (around 750 $\Omega.cm^2$), and a well-defined inductive loop at low frequency. This inductive phenomenon underlines the more significant occurrence of adsorbed molecules in the presence of NE on the steel surface, which can explain the higher charge transfer resistance (Amokrane et al., 2007; Vigdorovich et al., 2011).

During zinc electrodeposition, the steel surface is rapidly covered by zinc, and then the reduction of protons occurs on zinc surface. Thus, the effect of NE on the hydrogen evolution reaction was also characterized on zinc. As shown on Fig. 3a, the cathodic polarization curves highlight an inhibition of the H^+ reduction in the presence of NE on zinc as well. In fact, the current density of the first C1 broad peak, corresponding to the formation of hydrogen adsorbed species, significantly decreases (Fig. 3a) with NE concentration. Simultaneously, the current density C3 of hydrogen gas reduction is lowered, leading to an increase in the cathodic overpotential of hydrogen evolution, as measured in galvanostatic conditions in Fig. 3b. As noted on steel surface, this result suggests that the adsorbed species of nettle extracts act by blocking the active sites for the hydrogen reduction process, mainly caused by a partial coverage of the metal surface by molecules constituting the extract. The extract concentration of 1.5 $g\,L^{-1}$ seems to be optimal for the inhibition of hydrogen evolution on both steel and zinc surfaces.

3.2. Zinc electrodeposition with addition of nettle extract

Zinc electrodeposition was carried out in the plating bath containing the supporting electrolyte (0.1 M Na_2SO_4, 0.2 M H_3BO_3) and 0.1 M $ZnSO_4$ at pH = 2, without NE and with addition of 1.5 $g\,L^{-1}$ of NE. The corresponding cathodic polarization curves on steel are displayed in Fig. 4. At low cathodic potential, until −1450 mV, the C1 low measured cathodic current density is assigned to the formation of hydrogen and zinc adsorbed species on steel surface without crystallization of bulk metallic zinc, as mention ed. by many authors (Gomes and da Silva Pereira, 2006a; Salles et al., 2011). Between −1450 mV and − 1600 mV, the C′2 current density shoulder corresponds to the beginning of the reduction of Zn^{2+} cations into zinc metal. Finally, the C3 cathodic current density increase is due to Zn^{2+} and H^+ reduction. Similarly to the polarization curves on steel without zinc cations (Fig. 1a), NE addition firstly lowers the current density associated to hydrogen adsorption, and thus decreases the hydrogen evolution at high cathodic polarization beyond −1600 mV.

Depending on the potential scan rate, cathodic polarization current density values show that the electrochemical processes rely on the diffusion of H^+ and Zn^{2+} in the electrolyte (Figs. 5 and 6).

As illustrated in Fig. 5, the maximum of cathodic current densities sharply increase with the scan rate while the peak potentials move more

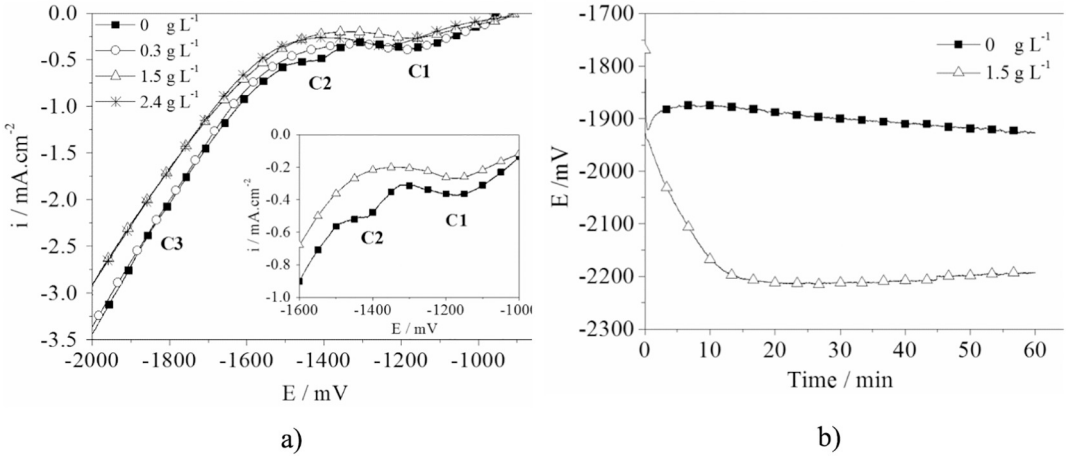

Fig. 1. Cathodic polarization curves (scan rate: 1 mV s^{-1}) (a) and chronopotentiometric curves at $i = -3$ mA.cm^{-2} (b) of steel in supporting electrolyte without Zn^{2+} ions with different NE concentrations.

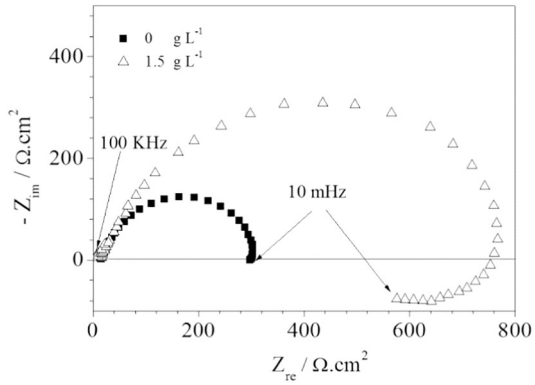

Fig. 2. Nyquist diagrams of steel in supporting electrolyte without Zn^{2+} ions without and with 1.5 g L^{-1} NE at open-circuit potential.

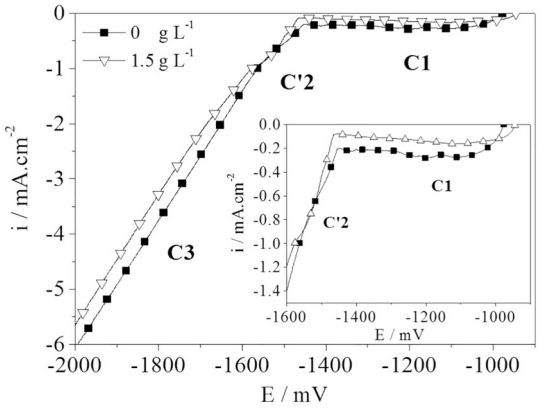

Fig. 4. Cathodic polarization curves of steel in the plating bath (with Zn^{2+} ions) without and with 1.5 g L^{-1} NE (scan rate: 1 mV s^{-1}).

negatively. More precisely, as interpreted in Fig. 6, the maximum of current densities i_p, on C1 and C′2 peaks, increases linearly as a function of the square root of the potential scan rate. This behavior confirms that both the zinc deposition (C′2) and the hydrogen adsorption (C1) reaction occur under diffusion control.

A relation between the cathodic peak current (i_p) and the scan rate (ν) for an irreversible process, leading to the formation of insoluble product is given by the following equation at 25 °C (Bard and Faulkner, 2001; Galus and Bryce, 1994): $i_p = 2{,}99.\ 10^5\ n\ \beta^{1/2}\ D^{1/2}\ C_0\ v^{1/2}$.

Where n is the number of electrons transferred, β is the cathodic charge transfer coefficient (β = 0.5 (Zhang and Hua, 2009)), D is the diffusion coefficient of the species in $m^2 \cdot s^{-1}$, C_0 is the concentration of diffusing species in $mol.m^{-3}$ and ν is the scan rate in $V \cdot s^{-1}$.

From the slope of the linear fit of the experimental data presented in Fig. 6 and using previous equation, the apparent diffusion coefficient of zinc cations for the zinc deposit process on steel is reported in Table 1, around 1.5 10^{-11} $m^2 \cdot s^{-1}$, which is slightly lower than the one reported

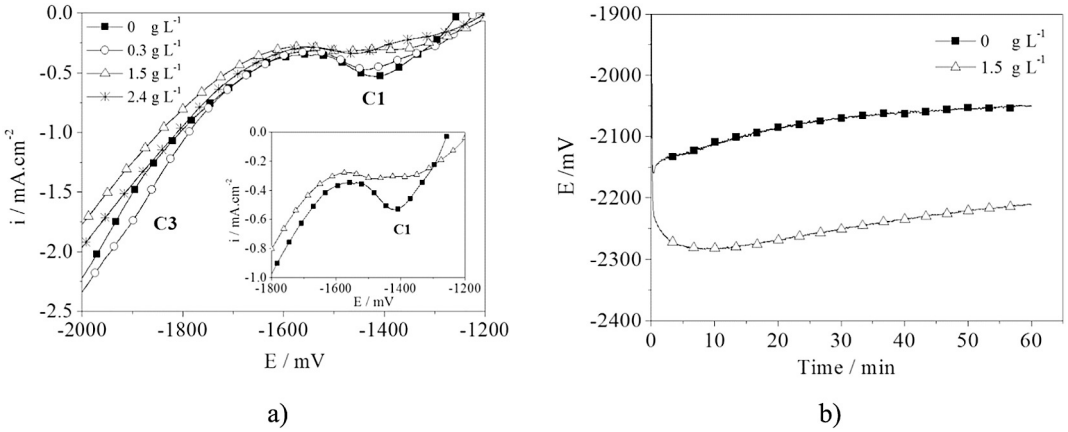

Fig. 3. Cathodic polarization curves (scan rate: 1 mV s^{-1}) (a) and chronopotentiometric curves at i = -3 mA.cm^{-2} (b) of zinc in supporting electrolyte without Zn^{2+} ions with different NE concentrations.

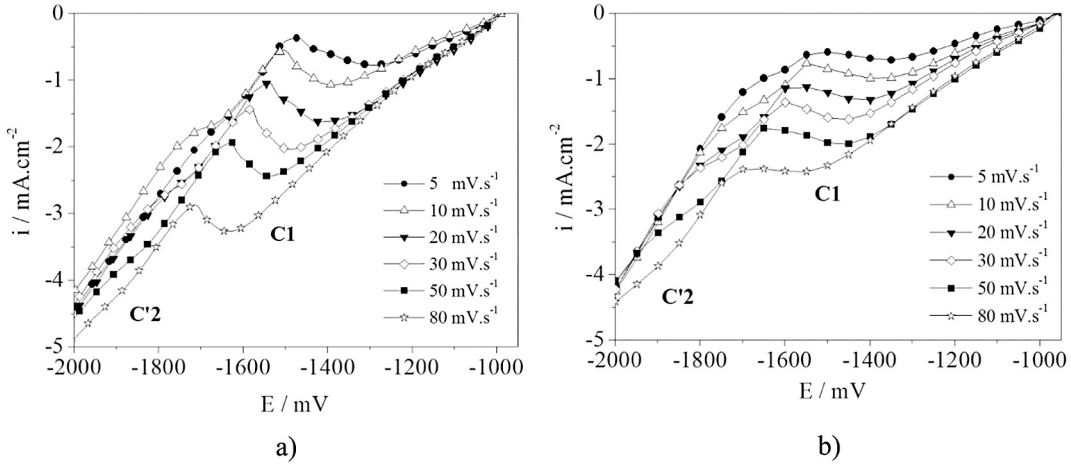

Fig. 5. Effect of potential scan rate on the cathodic polarization curves of steel in the plating bath (with Zn^{2+} ions), without (a) and with 1.5 g L^{-1} of NE (b).

in the literature for the bulk diffusion of Zn^{2+} cations in dilute sulfuric acid electrolyte (Guerra and Bestetti, 2006). This fact can be explained that Zn^{2+} diffusion near the steel surface is affected by the ionic strength of the electrolyte and diffusion layer in neighboring of steel surface

In presence of nettle extract, the apparent diffusion coefficient of Zn^{2+} cations during the zinc reduction process (C′2 peak) on steel is slightly affected.

On the contrary, the apparent diffusion coefficient of protons in electrolyte, close to 10^{-9} $m^2 \cdot s^{-1}$ (Leaist, 1984), is lowered by a factor 2 in the presence of extract. The decrease in protons coefficient diffusion is probably due to a change of conditions for access to the active sites on the steel substrate, due to the adsorption of molecules contained in the nettle extract.

3.3. Characterization of zinc deposits

Without and with 1.5 g L^{-1} of NE, surface of zinc deposits were observed by scanning electron microscopy after a potentiostatic process at −1700 mV (Fig. 7). In the present conditions of low zinc concentration and room temperature, the SEM micrograph of zinc deposit performed without NE (Fig. 7a) shows large aggregates of closely packed hexagonal zinc crystals, which grow perpendicularly to the substrate. Even if zinc crystals have a micrometer size, this kind of electrodeposit induces a relative high roughness and some problems with high thickness.

In the presence of nettle extract, a significant modification in the zinc deposits morphology is observed (Fig. 7b). The zinc grains are very fine and have a sub-micrometer size, almost nanometer, which makes the deposit very uniform and compact.

Table 1
Estimation of the apparent diffusion coefficient from the corresponding cathodic current peak on steel in the plating bath without and with 1.5 g L^{-1} of NE.

Estimated apparent diffusion coefficient/$m^2 \cdot s^{-1}$	Proton H^+ (peak C1)	Zn^{2+} cation (peak C2)
Without NE	$3.1\ 10^{-9}$	$1.5\ 10^{-11}$
With 1.5 g L^{-1} of NE	$1.8\ 10^{-9}$	$1.3\ 10^{-11}$

The preferential growth direction of zinc grain without additive is confirmed by the XRD pattern displayed in Fig. 8a. Actually, the strong (002) diffraction peak indicates a preferential orientation along the c axis perpendicular to steel surface, resulting from a minimization of the surface energy of the basal plane (Tanigushi et al., 2000; Matysina et al., 1992).

On the opposite, the XRD patterns of zinc deposit obtained with NE shows three main diffraction peaks, corresponding to the (100), (101), (110) planes of zinc structure, and the disappearance of the (002) diffraction peak at the same time, indicating a random orientation of the zinc grains with c-axis parallel to the steel surface. This effect has already been observed with other organic molecules, and could be attributed to an increase in the surface energy of (00c) planes, compared to (ab0) planes because of the specific adsorption of molecules of nettle extract (Gomes and da Silva Pereira, 2006b).

4. Conclusion

Throughout this study, the nettle (*Urtica dioica L.*) extract constitutes an interesting additive for zinc electrochemical reduction in

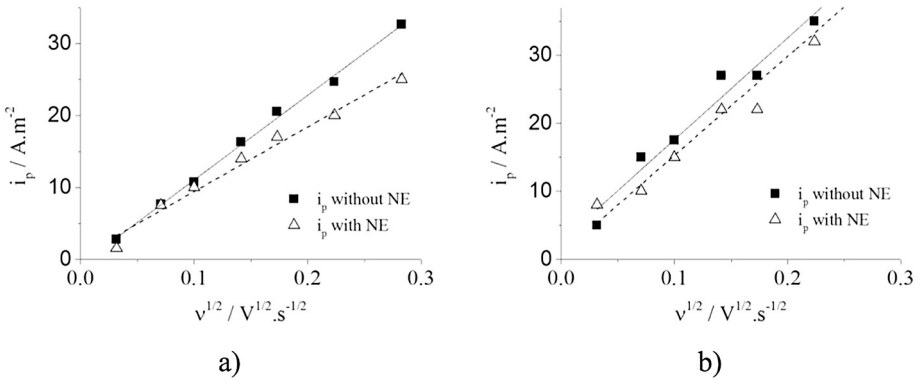

Fig. 6. Cathodic peak current (i_p) of the cathodic peak C1 (a) and C′2 (b) as a function of the sweep rate without and with 1.5 g L^{-1} of NE.

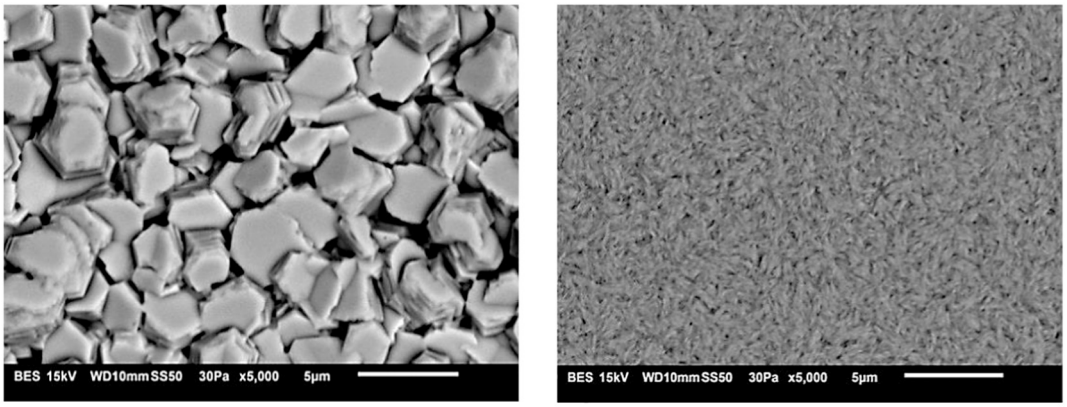

Fig. 7. SEM micrographs of zinc deposits at −1700 mV without (a), and with 1.5 g L^{-1} of NE (b).

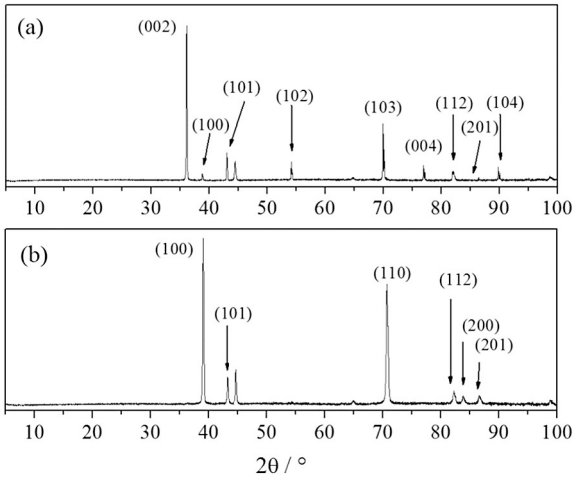

Fig. 8. X-ray patterns of zinc deposits at −1700 mV without (a), and with 1.5 g L^{-1} of NE (b).

acid sulfate electrolytes at room temperature and in relative low Zn^{2+} concentration, and can be applied for the zinc electrowinning or zinc coating processes.

The results show that the presence of nettle extract modifies both the electrochemical parameter of zinc electrodeposition, and the characteristic of the zinc deposit.

From the electrochemical point of view, the cathodic current density of proton reduction significantly decreases in the presence of NE from a concentration of 1.5 g L^{-1}. Especially, the extract lowers the proton adsorption on steel surface, which increases the cathodic overpotential of hydrogen evolution. Overall, the diffusion coefficient of protons is reduced by the presence of nettle extract in the electrolyte, likely due to the specific adsorption on active sites of some molecules contained in the extract. Nevertheless, the diffusion of Zn^{2+} cations is not significantly modified by the presence of extract.

The hypothesis of molecules adsorption on different sites on steel and zinc is also confirmed by the analysis of zinc coating. Indeed, in presence of nettle extract, the zinc deposit changes from a directed and coarse (00c) orientation without extract to a more random and finer (ab0) orientation with extract which is in good agreement with the SEM observations. The collection of molecules seems to favorably guide the electro crystallization of zinc in the exposed conditions.

Further studies are in progress to characterize and develop the practical use of nettle extract in industrial cell at room temperature and in low zinc concentrated electrolyte.

Declaration of Competing Interest

The authors declare that they have no known competing financial interests or personal relationships that could have appeared to influence the work reported in this paper.

References

Amokrane, N., Gabrielli, C., Ostermann, E., Perrot, H., 2007. Investigation of hydrogen adsorption–absorption on iron by EIS. Electrochim. Acta 53, 700–709. https://doi.org/10.1016/j.electacta.2007.07.047.

Bard, A.J., Faulkner, L.R., 2001. Electrochemical methods. In: Fundamentals and Applications, 2nd ed. John Wiley & Sons, New York.

Casanova, T., Soto, F., Eyraud, M., Crousier, J., 1997. Hydrogen absorption during zinc plating on steel. Corros. Sci. 39 (3), 529–537. https://doi.org/10.1016/S0010-938X(97)86101-X.

Díaz-Arista, P., Meas, Y., Ortega, R., Trejo, G., 2005. Electrochemical and AFM study of Zn electrodeposition in the presence of benzylideneacetone in a chloride-based acidic bath. J. Appl. Electrochem. 35 (2), 217–227. https://doi.org/10.1007/s10800-004-6304-7.

Đurovic, S., Pavlic, B., Šorgic, S., Popov, S., Savic, S., Pertonijevic, M., Radojkovic, M., Cvetanovic, A., Zekovic, Z., 2017. Chemical composition of stinging nettle leaves obtained by different analytical approaches. J. Funct. Foods 32, 18–26. https://doi.org/10.1016/j.jff.2017.02.019.

Epelboin, I., Ksouri, M., Lejay, E., Wiart, R., 1975. A study of the elementary steps of electron-transfer during the electrocrystallization of zinc. Electrochim. Acta 20, 603–605. https://doi.org/10.1016/0013-4686(75)80012-0.

Gabe, D.R., 1997. The role of hydrogen in metal electrodeposition processes. J. Appl. Electrochem. 27, 908–915. https://doi.org/10.1023/A:1018497401365.

Galus, Z., Bryce, W.A.C., 1994. Fundamentals of Electrochemical Analysis, 2nd ed. Ellis Horwood, New York.

Gomes, A., da Silva Pereira, M.I., 2006a. Zn electrodeposition in the presence of surfactants part I. Voltammetric and structural studies. Electrochim. Acta 52, 863–871. https://doi.org/10.1016/j.electacta.2006.06.025.

Gomes, A., da Silva Pereira, M.I., 2006b. Pulsed electrodeposition of Zn in the presence of surfactants. Electrochim. Acta 51, 1342–1350. https://doi.org/10.1016/j.electacta.2005.06.023.

Guerra, E., Bestetti, M., 2006. Physicochemical properties of $ZnSO_4$-H_2SO_4-H_2O electrolytes of relevance to zinc electrowinning. J. Chem. Eng. Data 51, 1491–1497.

Kerby, R.C., Jackson, H.E., O'keefe, T.J., Wang, Y.M., 1977. Evaluation of organic additives for use in zinc electrowinning. Metall. Trans. B 8, 661–668.

Leaist, D.G., 1984. Diffusion in aqueous solutions of sulfuric acid. Can. J. Chem. 62, 1692.

Loto, C.A., Olofinjana, A., Loto, R.T., 2014. Effect of *Manihot esculenta* C. leaf extract additive on the zinc electroplating on mild steel in acid chloride solution. Int. J. Electrochem. Sci. 9, 3746–3759.

Matysina, Z.A., Chuprina, L.M., Zaginoichenko, S.Y., 1992. J. Phys. Chem. Solids 53, 167–174.

M'hiri, N., Veys-Renaux, D., Rocca, E., Ioannou, I., Boudhrioua, N.M., Ghoul, M., 2016. Corrosion inhibition of carbon steel in acidic medium by orange peel extract and its main antioxidant. Corros. Sci. 102, 55–62. https://doi.org/10.1016/j.corsci.2015.09.017.

Mirkova, L., Maurin, G., Krastev, I., Tsvetkova, C., 2001. Hydrogen evolution and permeation into steel during zinc electroplating; effect of organic additives. J. Appl. Electrochem. 31, 647–654.

Mouanga, M., Ricq, L., Ismaili, L., Refouvelet, B., Berçot, P., 2007. Behaviour of coumarin in chloride bath: relationship with coumarin influence on zinc electrodeposition. Surf. Coat. Technol. 201, 7143–7148. https://doi.org/10.1016/j.surfcoat.2007.01.022.

Mouanga, M., Ricq, L., Berçot, P., 2008. Electrodeposition and characterization of zinc–cobalt alloy from chloride bath; influence of coumarin as additive. Surf. Coat. Technol. 202, 1645–1651. https://doi.org/10.1016/j.surfcoat.2007.07.023.

Salles, R.C.M., de Oliveira, G.C.G., Díaz, S.L., Barcia, O.E., Mattos, O.R., 2011. Electrodeposition of Zn in acid sulphate solutions: pH effects. Electrochim. Acta 56, 7931–7939. https://doi.org/10.1016/j.electacta.2010.12.026.

Scott, A.C., Pitblado, R.M., Barton, G.W., Ault, A.R., 1988. Experimental determination of the factors affecting zinc electrowinning efficiency. J. Appl. Electrochem. 18, 120–127.

Sorour, N., Zhang, W., Ghali, E., Houlachi, G., 2017. A review of organic additives in zinc electrodeposition process (performance and evaluation). Hydrometallurgy 171, 320–332. https://doi.org/10.1016/j.hydromet.2017.06.004.

Tanigushi, T., Sassa, K., Yamada, T., Asai, S., 2000. Control of crystal orientation in zinc electrodeposits by imposition of a high magnetic field. Mater. Trans. JIM 41 (8), 981–984. https://doi.org/10.2320/matertrans1989.41.981.

Trejo, G., Ruiz, H., Ortega Borges, R., Meas, Y., 2001. Influence of polyethoxylated additives on zinc electrodeposition from acidic solutions. J. Appl. Electrochem. 31, 685–692. https://doi.org/10.1016/j.electacta.2019.02.090.

Vigdorovich, V.I., Tsygankova, L.E., Balybin, D.V., 2011. Influence of guanidine on kinetics of hydrogen evolution reaction on iron and its diffusion through steel membrane in acidic chloride media. J. Electroanal. Chem. 653, 1–6. https://doi.org/10.1016/j.jelechem.2011.01.026.

Youssef, K.S., Koch, C.C., Fedkiw, P.S., 2004. Improved corrosion behavior of nanocrystalline zinc produced by pulse-current electrodeposition. Corros. Sci. 46, 51–64. https://doi.org/10.1016/S0010-938X(03)00142-2.

Zaabar, A., 2015. Electrodéposition, par voltampérométrie et cémentation, des métaux cuivre et zinc en présence d'extrait de la plante d'ortie (*Urtica dioica L.*). In: Application de L'extrait à la Corrosion. University of Bejaia Doctorat thesis.

Zaabar, A., Aitout, R., Makhloufi, L., Belhamel, K., Saidani, B., 2014. Inhibition of acid corrosion of mild steel by aqueous nettle extracts. Pigm. Resin Technol. 43, 127–138. https://doi.org/10.1108/PRT-11-2012-0078.

Zhang, Q.B., Hua, Y., 2009. Effect of $Mn2+$ ions on the electrodeposition of zinc from acidic sulphate solutions. Hydrometallurgy 99, 249–254.